The Journal of the Korean Society of
Coastal and Ocean Engineers
Vol. 6, No. 3, pp. 298~308, September 1994

A Numerical Modeling Study on the Interannual Variability in the Gulf of Alaska
알라스카 灣의 經年變化에 대한 數値模型 實驗

In Kweon Bang* and Zygmunt Kowalik**
方仁權* · 지그문트 코발릭**

Abstract □ Ocean circulation in the Northeast Pacific Ocean is simulated using a high-resolution primitive equation numerical model with realistic bottom topography. The goal is to explain better the details of observed interannual variability of the circulation in the Gulf of Alaska. Our numerical model suggests that there is no seasonal shift in the Alaska gyre and that the interannual variability, reported earlier, is most likely the result of embedded mesoscale eddies in the dynamic topography. Such eddies have been observed in hydrographic, satellite-tracked drifters and altimeter data from the Gulf of Alaska.

要 旨 : 북서태평양의 해수순환을 원시방정식 수치모형을 이용하여 재현하여 알라스카 만에서 관측된 해수순환의 경년변화에 대한 설명을 시도하였다. 모형 결과에 의하면 알라스카 gyre의 계절적 위치 변동은 없으며, 관측된 경년변화는 중규모 와류가 역학심도 계산에 영향을 미친 결과로 보인다. 이러한 중규모 와류는 수온 염분 관측, 부표추적 실험, 그리고 인공위성에 의한 해수면 관측에서도 관측되었다.

1. INTRODUCTION

The Gulf of Alaska contains the eastern part of the North Pacific subarctic gyre; a part of the general North Pacific subarctic/subtropical circulation system. The subarctic boundary, which separates the North Pacific subarctic gyre from the subtropical gyre, lies at about 40° N. The Subarctic Current, formed near Asia, flows eastward along this subarctic boundary and divides into the Alaska Current and the California Current near the west coast of North America. The northward flowing Alaska Current becomes a narrow and swift western boundary current known as the Alaska Stream as it turns to the southwest near the Kodiak Island. Thomson's vorticity analysis (1972) demonstrated that the β-effect is sufficiently large for the Alaska Stream to be a western boundary current. The Alaska Stream flows southwestward along the Alaska Peninsula and the Aleutian Islands until a portion of it recirculates into the gulf and rejoins the eastward flowing Subarctic Current. The remainder of the Alaska Stream continues to the west or enters the Bering Sea through the Aleutian Island passes.

Large variations in the flow of the Alaska Stream have been observed: for example, the transport relative to 1,500 db at about 176° W ranges from 5 Sv to 14 Sv according to Favorite *et al.* (1976). There have also been observations of an offshore shift of Alaska Stream from its normal position. For example, a 185 km shift occurred at 155° W in winter 1962 and a 280 km shift at 162° and 155° W in February and March 1967 with counter currents formed inshore at both times (Favorite *et al.* 1976). Reed *et al.* (1980) mentioned possible meanders and changes in the coastal current as an exp-

*韓國海洋研究所 海洋物理研究部 (Physical Oceanography Division, Korea Ocean Research and Development Institute, Ansan P.O. Box 29, 425-600, Korea)
**알라스카 대학 해양연구소 (Institute of Marine Scier ·, U. ersity of Alaska Fairbanks, Fairbanks, Alaska 99701, U.S.A.)

lanation for the variability in the Alaska Stream and recognized the need of a nonlinear model with stratification, topography, and β-effect.

An apparent shift of the Alaska Gyre was observed in the summers of 1958 and 1981 (Reed 1984; Royer and Emery 1987). Reed (1984) suggested that the anomalous conditions were the result of unusually weak wind stress forcing over the gulf in the three months or so prior to the time of observations. Cummins' numerical model results (1989) agree with Reed's observations (1984) by noticing the seasonal east-west shift of the gyre in his numerical results. Royer and Emery (1987) disputed this explanation and suggested an interaction of the eastward flowing North Pacific Current (Subarctic Current) with a group of seamounts near 51° N and 145° W as an alternative. According to Royer and Emery (1987) the shift of the gyre occurs when the North Pacific Current flows far north of its normal position and is deflected by the seamounts resulting in the westward shift of the Alaska Current.

Another possible cause of the circulation changes are mesoscale eddies. Ocean eddies have dominant temporal scales of weeks to months and spatial scales of tens to hundreds of kilometers. They commonly include a variety of variable flows such as meandering and filamenting of intense currents, semi-attached and cast-off rings, vortices, planetary waves, topographic waves and wakes (Robinson 1983). A well-documented feature in the Gulf of Alaska is an eddy observed offshore of Sitka at about 138° W, 57° N. Tabata (1982) described this eddy using 1954-1967 hydrographic data and the eddy was also detected with drifting buoys (Kirwan *et al.* 1978). The feature known as the Sitka eddy is about 200 to 300 km in horizontal diameter and extends to at least 2,000 m depth and has a transport of 5-8 Sv. It propagates westward with speeds greater than 1.5 km/day and persists 10-17 months. An anticyclonic eddy northwest of Sitka eddy and three cyclonic eddies along 55°N were also observed in February of 1967 by Roden (1969).

As an explanation of Sitka eddy Willmott and Mysak (1980) succeeded in producing an eddy-like structure from the reflection of a very low frequency Rossby waves by coastline. Tabata (1982) argued that topography should play an important role in the recurrence of Sitka eddy at the same location. In Cummins and Mysak (1988) an eddy appears at about the same location and they attributed the baroclinic instability of the Alaska Current for a generating mechanism.

Observations of long-period baroclinic Rossby waves in this region have been made by White and Tabata (1987). They used anomalies in the depth of $\sigma_t=26.8$ surface along Line P (50°N, 145° W to Vancouver Island) and concluded that the waves had periods of 1-5 years and were correlated to ENSO events. They also mentioned wind resonance as a possible explanation (White 1982) for the amplification of signal westward.

Several numerical models have been used to simulate the circulation in the Gulf of Alaska. Most recently, Cummins and Mysak (1988) and Cummins (1989) used an eddy-resolving quasi-geostrophic (QG) numerical model for the climatological mean and seasonal cycle circulation studies. They found that bathymetry plays an important role in the suppression of the seasonal variation in the volume transport of the Alaska Stream. Cummins (1989) also remarked that the abnormal shift of the Alaska gyre might result from variations in the integrated strength of the wind stress curl over the gulf.

The Gulf of Alaska was included in some larger scale numerical modeling studies of the North Pacific (Huang 1978, 1979; Hsieh 1987), but their coarse resolution made it difficult to comprehend the full dynamical effects of the Aleutian Islands and bottom topography on the Alaska gyre. Hsieh (1987) used an 1°×1°×6 (vertical levels) primitive equation model to study the seasonal circulation in the North Pacific and yielded unrealistic seasonal variations in the Gulf of Alaska, probably as a result of low vertical resolution.

Although the results by Cummins and Mysak (1988) and Cummins (1989) have led to a better understanding of the seasonal circulation in the Gulf of Alaska, QG models have limitations. QG theory assumes that the Rossby number, bottom relief, and the displacement of the interface are small. Furthermore, no thermohaline forcing is possible in the QG model. We here employed numeri-

cal model based on the primitive equations to excite mesoscale eddies and study their roles in the circulation of the Gulf of Alaska. In this study, a high resolution model is used which does not assume any of the above approximations used in the QG model and is capable of thermohaline forcing. Unlike Hsieh (1987), many vertical layers will be employed to include the effect of bottom topography.

2. NUMERICAL MODEL

Semtner's version (1974) of Bryan's (1969) primitive equation model is used in this study. This model adopts hydrostatic, Boussinesq, and rigid-lid approximations in a spherical coordinate system. Details of the numerical formulation and methods of finding solutions are in Semtner (1974).

The boundary conditions of momentum at the ocean surface and bottom are

$$\rho_o \kappa \frac{\partial \vec{u}}{\partial z} = \vec{\tau}_w, \text{ at } z=0,$$
$$\rho_o \kappa \frac{\partial \vec{u}}{\partial z} = \vec{\tau}_b, \text{ at } z=-H \quad (1)$$

where z is positive upwards, $\vec{u}$ is the horizontal velocity vector, ρ_o is the mean water density, κ is the vertical eddy viscosity. $\vec{\tau}_w$ and $\vec{\tau}_b$ are wind stress and bottom stress vectors, respectively. For temperature, T, and salinity, S, a no flux boundary condition is used at the ocean surface (z=0) and bottom (z=−H) which is

$$\rho_o \kappa \frac{\partial (T,\ S)}{\partial z} = 0 \quad (2)$$

Biharmonic friction (Cox 1984) is used for horizontal friction and diffusion to resolve eddies. Biharmonic friction has an advantage over Laplacian friction in that it dissipates small scale motions more quickly than large scale motions so that the frictional effects on the mesoscale eddies and large scale circulation can be much smaller while still maintaining computational stability (Pond and Pickard 1983). For this reason it is sometimes called 'scale-selective friction'. A boundary condition on temperature and salinity which incorporates biharmonic diffusion is

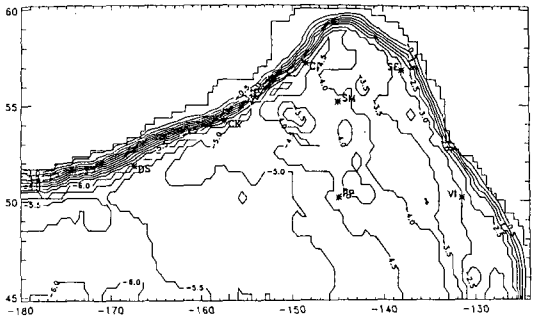

Fig. 1. Northeast Pacific bottom topography used in the model. Seven monitoring points are marked by asterisk (VI: Vancouver Island, PP: Papa, CI: Cook Inlet, SE: Sitka Eddy, SM: Seamount, CK: Chirikof Island, and DS: Downstream).

$$\frac{\partial \sigma}{\partial n} = 0, \quad \frac{\partial}{\partial n} \nabla^2 \sigma = 0 \quad (3)$$

where σ is either temperature or salinity and n is normal direction to the boundary. For the momentum, no-slip boundary condition is used, i.e.,

$$\vec{u} = 0, \quad \nabla^2 \vec{u} = 0 \quad (4)$$

The model domain is closed by artificial walls at the western (180°) and southern (45° N) boundaries (Fig. 1). These walls block the water exchange and interaction of the Gulf of Alaska with the rest of North Pacific. Appropriate treatments on the walls are needed to minimize the possible effects of this isolation of the gulf. The presence of the wall in the model would force the Alaska Stream to flow southward along the wall and reenter the interior as the Subarctic Current. This transformation of the Alaska Stream to the Subarctic Current might be acceptable because no in- and outflows are prescribed at the western boundary in the model. However, waves and eddies propagating from the interior would also be reflected by the wall or reenter the interior resulting in the contamination of the interior circulation.

A high friction region (so-called 'sponge layer') is commonly implemented near the artificial boundary. In the sponge layer, the incoming waves and eddies are dissipated by the high friction to prevent them from contaminating the interior (Cummins and Mysak 1988). Usually, friction coefficients are increased gradually from an interior value to the

high value in the sponge layer. In this computation, however, the Laplacian diffusion scheme with a constant coefficient over 10 grid points adjacent to the artificial western wall was adopted after various schemes had been tried. The Laplacian diffusion is chosen because it dissipates mesoscale motions more effectively than the biharmonic diffusion.

The southern boundary is located near the zero wind stress curl line and the current direction at this latitude (45° N) is nearly zonal. A problem was noted at the southern boundary. Anticyclonic vortices were generated from the wall and anticyclonic circulation eventually filled the eastern half of the gulf. The anticyclonic eddies were found to be generated by a strong eastward current formed as the strong westerly wind establishes downwelling along the southern boundary. As a remedy to this problem, a 'linear zone' is established over 2 grid points from the southern boundary where the advection terms are removed from both momentum and temperature (salinity) equations. This linear zone ensures no generation of anticyclonic eddies from the wall by eliminating a unrealistic downwelling responsible for the horizontal density gradient from which the anticyclonic eddies extract energy for their growth.

The spin-up time of the baroclinic ocean is considerably longer than that of the barotropic ocean and an equilibrium is achieved after the passage of baroclinic Rossby waves. However, the speed of first baroclinic Rossby wave is on the order of 0.01 m/sec at high latitude (Lighthill 1969) and it takes a decade for the baroclinic Rossby wave to cross the Gulf of Alaska at this speed. Therefore, it takes more time to spin up the baroclinic ocean at high latitudes than near the equator where the spin-up time is on the order of months.

Thermohaline information at the ocean surface takes an order of thousand years to reach the deep portion of a ocean because of the small vertical diffusivity. The use of longer time step for the density field is one way of speeding up the spin-up process. Bryan (1984) further extended this method by using longer time steps in deep layers. However, this approach of different time stepping is valid only for a steady-state solution.

Semtner and Chervin (1988) adopted the robust-diagnostic method (Sarmiento and Bryan 1982) for a fast spin-up to the observed density field in their world ocean circulation model. The model density field is forced to the observed density field by the help of a Newtonian type forcing term in the temperature and salinity equations.

$$-\frac{1}{\gamma}(T-T_o) \text{ and } -\frac{1}{\gamma}(S-S_o) \tag{5}$$

where T_o and S_o are the observed values and γ is the restoring time scale. When γ is small, the predicted temperature (T) is almost equal to the observed temperature (T_o) and the model becomes a pure diagnostic model. When γ is large, this term is negligible and the model becomes a prognostic model. For example, Semtner and Chervin (1988) spun up the world ocean in a decade by gradually increasing the restoring time scale through time. After the spin-up process, Semtner and Chervin (1988) removed the robust-diagnostic term from layers in the upper 1,000 m for a study of transient motions. A short time scale (a month) was kept throughout the integration in the surface layer to keep the surface density close to the observed value as a thermohaline forcing.

The robust-diagnostic approach is also adopted for the spin-up process in our study. One year of restoring time scale is used during the first two years in all layers except for the surface layer where a restoring time scale of 30 days is kept throughout the integration. Wind stress is linearly increased during the first year and remains constant after reaching its normal strength at the end of the first year. The initial conditions are horizontally homogeneous temperature and salinity fields and no motion. Temperature and salinity data of Levitus (1982) were used as the oceanographic observation. For the determination of density from temperature and salinity, a polynomial expression of Friedrich and Levitus (1972) is used. Resolution of 30′ (zonal)×20′ (meridional) with 20 vertical layers is adopted. The horizontal resolution is 31 km (at 55° N)×37 km and is larger than 25 km used by Cummins and Mysak (1988).

Abrupt changes in depth, such as those found

across a trench, can cause numerical instabilities in a primitive equation model (Ramming and Kowalik 1980; Killworth 1987). A certain amount of topographic smoothing is necessary therefore to ensure numerical stability, although some dynamics are lost. A smoothed depth distribution was obtained from 5'-interval depth data both in longitude and latitude. The raw data were smoothed by 9-point Shapiro filter (Shapiro 1970), subsampled every 30 in longitude and 20 in latitude, and smoothed once more by the same filter. Seamounts and the Aleutian trench, which are considered dynamically important in the Gulf of Alaska, remain resolved with this resolution (Fig. 1).

Forty three years (1946-1988) of monthly mean sea level atmospheric pressure of Fleet Numerical Oceanography Center were used for the computation of wind stress. Geostrophic winds were computed from derivatives of monthly mean sea level pressure using natural cubic spline interpolation (Cheney and Kincaid 1985). Wind directions were rotated 15° counter-clockwise and wind speeds were reduced 30% to compensate for the effect of friction (Willebrand 1978; Luick *et al.* 1987). Next, wind stresses were computed applying Garratt's (1971) formula for drag coefficient.

Wind stress curl appears as a forcing term in the vorticity equation of the vertically integrated transport. Therfore, a wind-driven circulation can be understood more easily in terms of the wind stress curl than the wind stress, although the latter is used to force the model ocean in the computation. Annual mean and seasonal range of the wind stress curl computed from the wind stress in the Gulf of Alaska is shown in Fig. 2. Maximum positive wind stress curl is about 3×10^{-8} dyn/cm^3 and is located at 58° N, 140° W. In general, the wind stress curl used in this computation is higher in the region north of 55° N and lower to the south of 55° N compared to Willebrand (1978).

3. RESULTS

The circulation computations are carried out for 28 years with annual mean forcing. Biharmonic coefficients are 1×10^{19} and 6×10^{19} cm^4/sec for momentum and diffusion, respectively. The domain-averaged kinetic energy shows a state close to equilibrium after 10 years of integration.

The time series of the stream function at various locations in the Northeast Pacific reveal the spatial variabilities of the interannual fluctuations in the

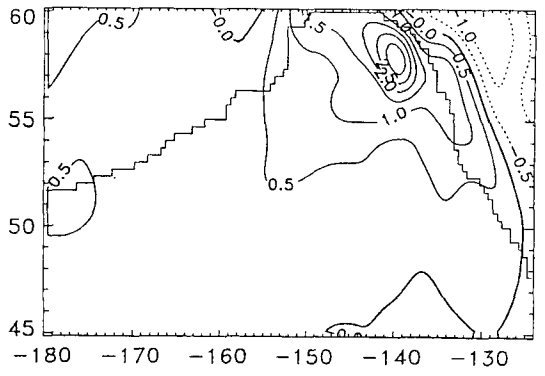

Fig. 2. Annual mean wind stress curl. Unit is 1×10^{-8} dyn/cm^3.

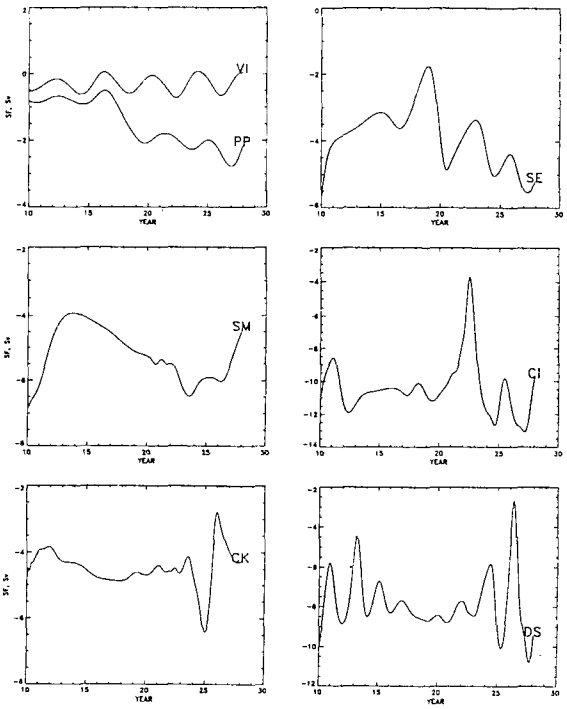

Fig. 3. Time series of stream function at seven monitoring points (see Fig. 1 for the locations).

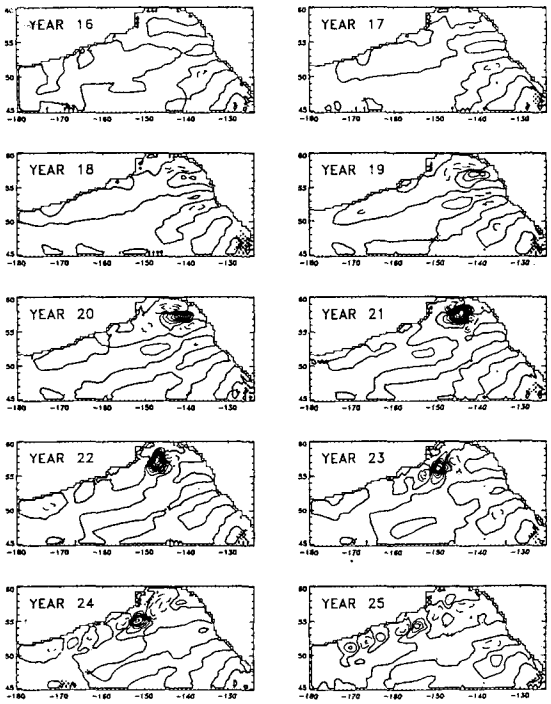

Fig. 4. Demeaned and detrended stream function for year 16-25. Contour interval is 1 Sv and negative contour lines are denoted by dashed line.

gulf (Fig. 3). At Vancouver Island (VI) and Papa (PP) (Fig. 1), the fluctuations are regular in time and have a period of about 4 years (Fig. 3). The range of the fluctuations is small at both locations and is less than 1 Sv.

At Sitka (SE), Cook Inlet (CI) and Chirikof Island (CK), the fluctuations are associated with the passages of eddies and can be better understood by contour plots of the perturbation stream function (Fig. 4). A most prominent feature is a high near 57° N, 140° W in year 20. Before year 20, this anticyclonic eddy is not strong enough to be easily distinguished from other highs or lows. It propagates westward to near Kodiak Island and from there propagates southwestward along the shelf with the Alaska Stream. The eddy begins to weaken during year 23 and eventually becomes nondistinguishable from other eddies. Its passage is detected as peaks in the time series of the stream function at monitoring points (Fig. 3). The first peak in year 19 at SE and a peak in year 22 at CI are caused by the passage of this anticyclonic eddy. It reaches CK

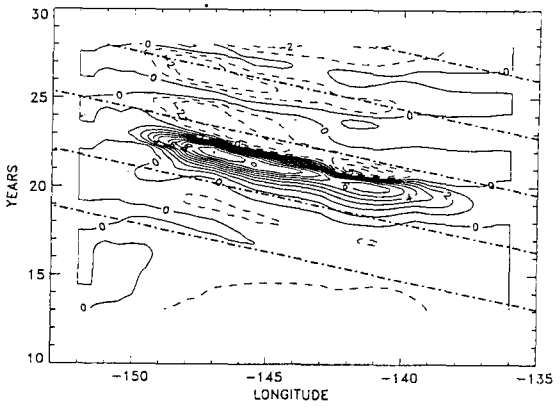

Fig. 5. Contour plot of the detrended stream function in time-longitude space along 57° 10′ N. Superimposed are lines of constant speed of 0.6 cm/sec.

in year 26 but the integration was not long enough to detect it downstream (DS). There are two more peaks with ever decreasing amplitudes at SE. They occur in years 23 and 26 and propagate to CI to be recorded as peaks in year 25 and 28, respectively.

The period of the occurrence of these anticyclonic eddies at SE is 3-4 years and the propagation time to CI is 2-4 years. This can be summarized by a time-longitude plot along 57° 10′ N (Fig. 5) which is close to the latitude where both points (SE and CI) are located. From this figure, one can estimate the westward propagation speed of these eddies as about 0.6 cm/sec. The estimate of the zonal wavelengtth is 550-750 km from the period of 3-4 years and the phase speed of 0.6 cm/sec. The propagation speed is on the order of those of the baroclinic Rossby waves (Lighthill 1969) whose maximum westward propagation speed is given by

$$C=\frac{\beta g h}{f^2} \tag{6}$$

where β is the meridional gradient of the Coriolis parameter $f=2\Omega\sin\varphi$, Ω=angular rate of rotation of earth, φ is the latitude, g is the acceleration due to gravity and h is the effective depth. An effective depth of 0.73 m at 57° N is obtained from the westward propagation speed of 0.6 cm/sec by (6) and agrees well with the effective depth of 0.67 m which was estimated by approximating the continuous vertical profile of sigma-t by 3 layers.

The anticyclonic eddies which propagate from Sitka (site SE) to near Kodiak Island can be identified as the Sitka eddies. Tabata (1982) estimates the westward propagation speed of Sitka eddy to be more than 1.7 cm/sec and the transport associated with it 5-8 Sv. The estimate of the size of Sitka eddy (Tabata 1982) is 200-300 km and agrees well with the size of the anticyclonic eddies in the model (the size of an eddy is half its wavelength, 550-750 km in this case). Gower (1989) also reports the observation of eddies in the eastern gulf in Geosat altimetry data from November 1986 to June 1988 and concludes that the propagation is primarily to the west at a speed of about 1.3 cm/sec. There is a discrepancy between the observations and the model results; the propagation speed is only about half of the observed value. There are two possible explanations for this discrepancy; 1) the model effective depth is about half of that of the Gulf of Alaska when the observations were made, 2) the propagation speed is a sum of advection by mean current and the intrinsic speed, and the speed of the model mean current is smaller than that of the Gulf of Alaska.

The propagation of anticyclonic eddies from near the coast of North America to the Alaska Stream provides an interesting possibility to interpret the abnormal shift of the Alaska gyre (Royer and Emery 1987). Royer and Emery (1987) and Reed (1984) report the disappearance of the Alaska Stream in the Cook Inlet line in summer 1981. As a possible cause of the shift, Reed (1984) suggests the change in the wind stress and Royer and Emery (1987) suggest the interaction of North Pacific Current with seamounts. Musgrave *et al.* (1992) observe a meander of the Alaska Stream in May 1988 and identify it as being caused by the arrival of an eddy originated from near Yakutat in January 1987 which was detected by Gower (1989). Musgrave *et al.* (1992) suggest the passage of anticyclonic eddies as an explanation of abnormal shift of the Alaska gyre. Reed and Stabeno (1989) also report observations of the disappearance of the Alaska Stream from its normal path for at least 3 months (April-June) in 1986 and '987 near Chirikof Island. It has been shown in this computation that the passage of anti-

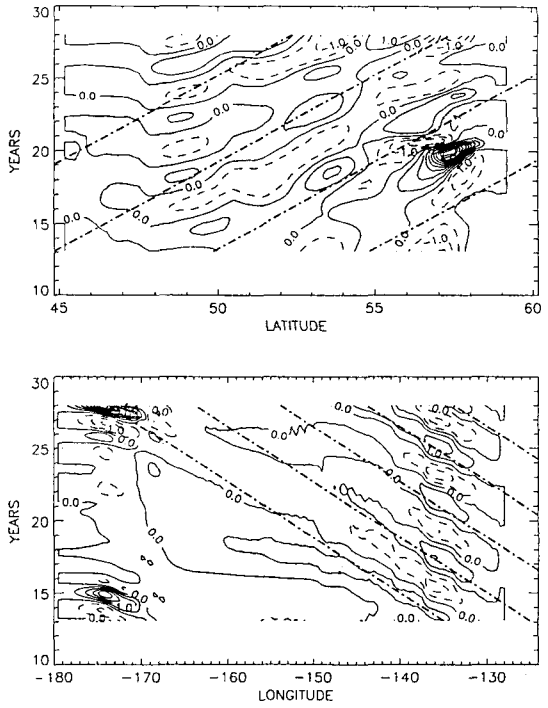

Fig. 6. Contour plots of the detrended stream functions in time-longitude space along 50° N and in time-latitude space along 140° W. Superimposed are lines of constant speed; 0.3 cm/sec for time-latitude plot and 0.6 cm/sec for time-longitude plot.

cyclonic eddies causes large decreases in the transport of the Alaska Stream at fixed points (Fig. 3). The model results agree with Musgrave *et al.* (1992), such that there is no large scale shift of Alaska gyre, only the passage of mesoscale eddies. Also, the disappearance of the Alaska Stream over the Cook Inlet line in summer 1981 could have been the result of the passage of anticyclonic eddy.

A series of oceanic lows and highs are elongated southwestward from the coast of North America (Fig. 4). As shown in the time-longitude and time-latitude plots of perturbation stream function of Fig. 6, the system propagates northwestward. The fluctuations in the region of 48° N-51° N and 130° W-140° W are regular in time and their period is about 4 years. This period was also seen in the time series of the stream function at VI and PP (Fig. 3). The region from the coast of North America to 145° W and south of 51° N can be delineated as the region with regular fluctuations with pe-

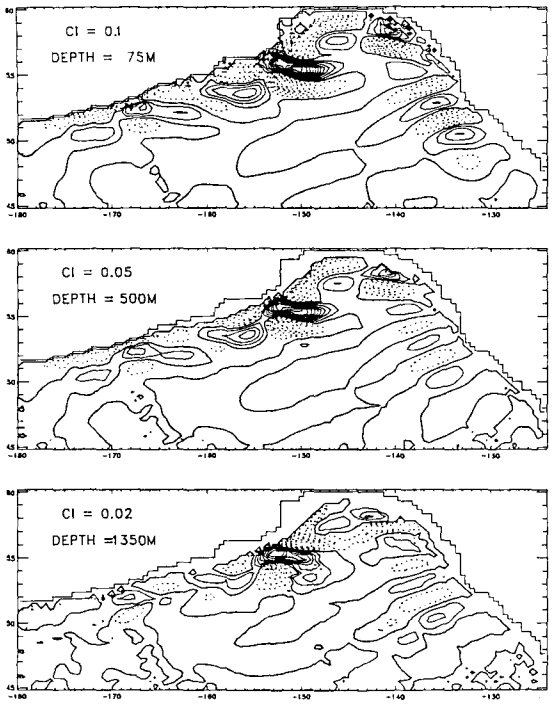

Fig. 7. Distributions of linear trend (cm/sec/month) in zonal velocities over 1 year in year 23-24 at three depths. Contour intervals (CI) and depths are indicated in the upper left corner of each figure. Solid lines represent positive trends.

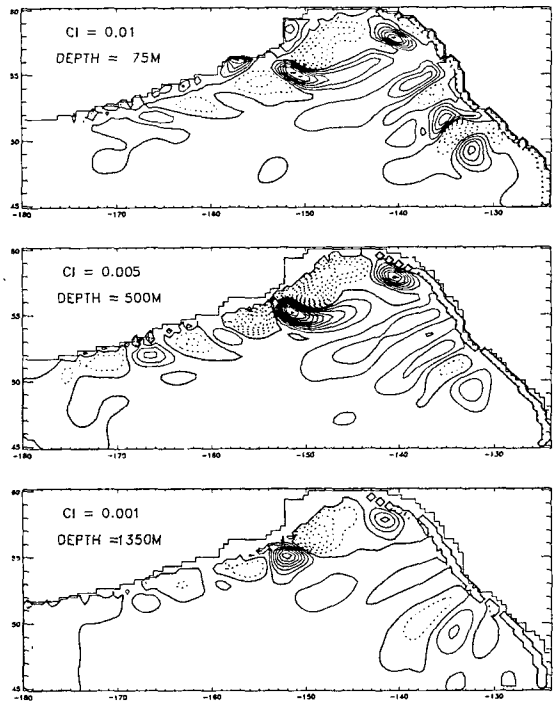

Fig. 8. Distributions of linear trend (℃/month) in temperatures over 1 year in year 23-24 at three depths. Contour intervals (CI) and depths are indicated in the upper left corner of each figure. Solid lines represent positive trends.

riods of about 4 years. The propagation speed of the eddies in this region estimated from Fig. 6 is about 0.6 cm/sec in both westward and northward directions. The northward propagation speed slows to only about 0.3 cm/sec in the region north of 55° N (upper panel of Fig. 6) and becomes zero near 58° N as the eddies approach the shelf. The eddies then propagate westward (Fig. 5).

Although the fluctuations farther north (>55° N) are not as regular as those in the southern region, one can estimate that the period is 3-4 years from the time series of stream function at SE (Fig. 3) which is located only a couple of degrees to the east of the longitude along which Fig. 6 is constructed. The most prominent anticyclonic eddy described above by the time series of stream function (Fig. 3) and the time sequence of perturbation stream function (Fig. 4) is also seen around 56°-58° N in year 20 (upper panel of Fig. 6). In this figure, one can also see that this eddy and two more succeeding eddies are actually the continuation of eddies formed farther south. Therefore, the Sitka eddy observed frequently near 57° N, 138° W (Tabata 1982) is not locally formed but it is formed farther to the south and has propagated to this latitude.

Next, we analyze velocities and temperatures at three depths. The linear trend is defined as the slope of the linear fit to the data over one year. It has the dimension of acceleration (cm/sec^2) if velocity is used. Positive and negative linear trends indicate eastward and westward accelerations, respectively. An anticyclonic eddy consists of the positive (eastward) northern half and the negative (westward) southern half. In Fig. 7, one can see that the eddies at a greater depth are ahead of the shallower ones all along the boundaries from the southeastern corner to the western end of the sloping boundary. Since the Alaska gyre flows in a counterclockwise sense, the eddies are aligned in the vertical direction in such a way that the mean potential energy is

released into the eddy energy (Pedlosky 1982).

The center of the positive trend in temperature corresponds to the center of the anticyclonic eddy (Fig. 8) and is located at the boundary between the positive and negative accelerations in velocity (Fig. 7). Since the anticyclonic eddy has a downwelling at its center and the positive tendency (increase) in temperature also indicates the downwelling, the trends in the velocity and temperature are consistent with the eddy dynamics. Spatial distributions of the linear trends in the zonal velocity and temperature indicate that these eddies are due to baroclinic instability.

4. DISCUSSION AND CONCLUSIONS

In this study, a series of numerical experiments have been carried out to simulate the ocean circulation in the Gulf of Alaska. A focus of this work is on the explanation of the abnormal shift of the Alaska gyre.

Eddies are the major contributor to the mesoscale variabilities in the gulf and they were interpreted as Rossby waves. We also have performed a computation (Bang 1991) for the flat-bottom case. There is a shift in the observed period of eddies from 70-80 days in flat-bottom case to 3-4 years in topographic case. The horizontal scale of the eddies also changes from about 250 km to 550-750 km. The eddies in the flat-bottom case are quite regular both in space and time and they are more like waves. In the topographic case, the anticyclonic eddy which was identified as the Sitka eddy looks like an isolated ring (or solitary Rossby wave) and maintains its identity for a long time (about 5-6 years) suggesting the importance of nonlinearities. Boning (1989) also finds that the vortices keep their identity for a much longer duration in the topographic case than in the flat-bottom case where they are quickly destroyed by wave radiation. Another interesting fact about the Sitka eddy is its rotation. Although local bottom topography could select the anticyclonic eddies preferentially, there is also a possibility that it is due to the asymmetry between anticyclonic and cyclonic vortices. Cushman-Roisin and Tang (1990) find that anticyclonic eddies are more robust than cyclonic eddies when a generalized geostrophic equation (the amplitude of the perturbation is not restricted to be small as in QG equation and can be as large as the water depth) is used. Their single-eddy numerical experiments show that an anticyclonic eddy keeps its identity for a longer time than a cyclonic eddy which breaks up quickly. This adds to the ability of the anticyclonic eddy to persist.

Satellite infrared images sometimes show mesoscale eddies in the Alaska Stream (Gower and Royer 1986). They appear as a series of crests and troughs along the Alaska Stream as in the flat-bottom case. One big difference between eddies from the model and the satellite images is in the length scale. The length scale of eddies in the satellite images (only about 50-100 km from crest to crest) is smaller than that (200-250 km) in the flat-bottom case. Although a strict comparison is not possible between them without more information (for example, period or propagation speed) on the satellite imaged eddies, one possible cause for the discrepancy in the length scale is our model grid size (about 37 km) which is not capable of resolving motions smaller than about 74 km (2 Δx). A higher resolution model will be needed to clarify this point.

White and Tabata (1987) identified signals with a period of 1-5 years in the isopycnals along the Line P and suggested the teleconnection to the El Nino as their source. In this study, however, similar signals with a period of 4 years were excited by the baroclinic instability of the Alaska Current. Therefore, it is possible that the signal observed by White and Tabata (1987) is also due to the baroclinic instability of the Alaska Current.

Cummins (1989) suggested that the abnormal shift of the Alaska gyre observed in 1981 (Reed 1984; Royer and Emery 1987) is an amplification of the seasonal shift of the gyre. However, Bang (1991) found no seasonal shift of gyre in the primitive equation model results. Reed *et al.* (1980) also found no clear evidence of seasonal cycle in the transport of the Alaska Stream.

The numerical approach discussed here answers several questions that have recently been generated from hydrographic observations. The source of mesoscale eddies observed in the northern Gulf of

Alaska appears to be instabilities in the Alaska Current on the eastern side of the Gulf of Alaska. These eddies are long-lived and takes tens of months to cross the gulf. They can disrupt the interpretations of hydrographic observations since their scale lengths are less than the section spacing. They are also probably important to the biology and chemistry of the region and should be considered in any future observation programs.

ACKNOWLEDGMENTS

We thank Dr. A.J. Semtner for making the code of his primitive equation, numerical model available to us. This study was supported by the National Science Foundation under grants OCE8608125 and OCE9012866. We thank Dr. T.J. Weingartner for his review of the manuscript. A generous offer of the computer time from San Diego Supercomputer Center was essential for this study.

REFERENCES

Bang, I., 1991. Numerical modeling study of the circulation in the Gulf of Alaska, Ph.D. thesis, University of Alaska Fairbanks.

Bang, I. and Kowalik, Z., 1994. A numerical modeling study on the seasonal variability in the Gulf of Alaska, *J. Korean Soc. Coastal and Ocean Engineers*, **6** (3), 309-325.

Boning, C.W., 1989. Influences of a rough bottom topography on flow kinematics in an eddy-resolving circulation model, *J. Phys. Oceanogr.*, **19**, 77-97.

Bryan, K., 1969. A numerical method for the study of the ocean circulation, *J. Comput. Phys.*, **4**, 347-376.

Bryan, K., 1984. Accelerating the convergence to equilibrium of ocean-climate models, *J. Phys. Oceanogr.*, **14**, 666-673.

Cheney, W. and Kincaid, D., 1985. *Numerical mathematics and computing*, 2nd ed. Brooks/Cole Publishing Company.

Cox, M.D., 1984. A primitive equation, 3--dimensional model of the ocean, GFDL Ocean Group Tech. Rep. No. 1.

Cummins, P.F., 1989. A quasi-geostrophic circulation model of the Northeast Pacific. Part II: Effects of topography and seasonal forcing, *J. Phys. Oceanogr.*, **19**, 1649-1668.

Cummins, P.F. and Mysak, L.A., 1988. A quasi-geostrophic circulation model of the Northeast Pacific. Part I: A preliminary numerical experiment, *J. Phys. Oceanogr.*, **18**, 1261-1286.

Cushman-Roisin, B. and Tang, B., 1990. Geostrophic turbulence and emergence of eddies beyond the radius of deformation, *J. Phys. Oceanogr.*, **20**, 97-113.

Favorite, F., Dodimead, A.J. and Nasu, K., 1976. Oceanography of the subarctic Pacific region, 1960-1971, International North Pacific Fisheries Commission Bulletin, 33.

Friedrich, H. and Levitus, S., 1972. An approximation to the equation of state for sea water, suitable for numerical ocean models, *J. Phys. Oceanogr.*, **2**, 514-517.

Garratt, J.R., 1977. Review of drag coefficients over oceans and continents, *Mon. Wea. Rev.*, **105**, 915-929.

Gower, J.F.L., and Royer, T.C., 1986. Gulf of Alaska/Aleutian Islands. In Nimbus-7 Coastal Zone Color Scanner Imagery for Selected Coastal Regions, Prepared by W.A. Hovis, E.F. Szajna and W.A. Bohan, NASA, Goddard Space Flight Center, 3-6.

Gower, J.F.L., 1989. Geosat altimeter observations of the distribution and movement of sea-surface height anomalies in the north-east Pacific, *In Oceans 89. Navigation, Remote Sensing, Underwater Vehicles/Explotation*, **3**, 977-981.

Hsieh, W.W., 1987. A numerical study of the seasonal cycle and its perturbations in the northeast Pacific Ocean, *Atmos. Ocean*, **25**, 375-386.

Huang, J.C.K., 1978. Numerical simulation studies of oceanic anomalies in the North Pacific Basin: The ocean model and the long-term mean state, *J. Phys. Oceanogr.*, **8**, 755-778.

Huang, J.C.K., 1979. Numerical simulation studies of oceanic anomalies in the North Pacific Basin. Part II: Seasonally varying motions and structures, *J. Phys. Oceanogr.*, **9**, 37-56.

Killworth, P.D., 1987. Topographic instabilities in level model OGCMs, Ocean Modelling (unpublished manuscript) No. 75, 9-12.

Kirwan, A.D., Jr., McNally, G.J., Reyna E. and Merrell, W.J., Jr., 1978. The near-surface circulation of the eastern North Pacific, *J. Phys. Oceanogr.*, **8**, 937-945.

Levitus, S., 1982. Climatological atlas of the world ocean, NOAA Prof. Paper 13.

Lighthill, M.J., 1969. Dynamic Response of the Indian Ocean to Onset of the Southwest Monsoon, *Philosophical Transactions of the Royal Society of London*, **A 270**, 371-390.

Luick, J.L., Royer, T.C. and Johnson, W.R., 1987. Coastal atmospheric forcing in the northern Gulf of Alaska, *J. Geophy. Res.*, **92**, 3841-3848.

Musgrave, D.L., Weingartner, T.J. and Royer, T.C., 1992. Circulation and hydrography in the northwestern Gulf of Alaska, *Deep Sea Res.*, **39**, 1499-1519.

Pedlosky, J., 1982. *Geophysical Fluid Dynamics*, Springer-Verlag.

Pond, S., and Pickard, G.L., 1983. *Introductory Dynamical Oceanography*, Pergamon Press.

Ramming, H.G., and Kowalik, Z., 1980. *Numerical Modelling of Marine Hydrodynamics*, Elsevier.

Reed, R.K., 1984. Flow of the Alaskan Stream and its variations, *Deep Sea Res.*, **31**, 369-386.

Reed, R.K., Muench, R.D. and Schumacher, J.D. 1980. On baroclinic transport of the Alaskan Stream near Ko-

diak Island, *Deep Sea Res.*, **27A**, 509-523.

Reed, R.K. and Stabeno, P.J., 1989. Recent observations of variability in the path and vertical structure of the Alaska Stream, *J. Phys. Oceanogr.*, **19**, 1634-1642.

Robinson, A.R., 1983. Overview and summary of eddy science. *Eddies in Marine Science*, A.R. Robinson, Ed., Springer-Verlag, 3-15.

Roden, G.I., 1969. Winter circulation in the Gulf of Alaska, *J. Geophy. Res.*, **74**, 4523-4534.

Royer, T.C. and Emery, W.J., 1987. Circulation in the Gulf of Alaska, 1981, *Deep Sea Res.*, **34**, 1361-1377.

Sarmiento, J.L., and Bryan, K., 1982. An ocean transport model for the North Atlantic, *J. Geophy. Res.*, **87**, 394-408.

Semtner, A.J., 1974. An oceanic general circulation model with bottom topography, Numerical Simulation of Weather and Climate, Tech. Rep. No. 9, Dept. Meteor. UCLA, 99p.

Semtner, A.J. and Chervin, R.M., 1988. A simulation of the global ocean circulation with resolved eddies, *J. Geophy. Res.*, **93**, 15502-15522.

Shapiro, R., 1970. Smoothing, filtering, and boundary effects, *Rev. Geophys. Space Phys.*, **8**, 359-387.

Tabata, S., 1982. The anticyclonic, baroclinic eddy off Sitka, Alaska, in the northeast Pacific Ocean, *J. Phys. Oceanogr.*, **12**, 1260-1282.

Thomson, R.E., 1972. On the Alaska Stream, *J. Phys. Oceanogr.*, **2**, 363-371.

White, W.B., 1982. Travelling wavelike mesoscale perturbations in the North Pacific Current, *J. Phys. Oceanogr.*, **12**, 231-243.

White, W.B. and Tabata, S., 1987. Interannual westward-propagating baroclinic long-wave activity on Line P in the eastern midlatitude North Pacific, *J. Phys. Oceanogr.*, **17**, 385-396.

Willebrand, J., 1978. Temporal and spatial scales of the wind field over North Pacific and North Atlantic, *J. Phys. Oceanogr.*, **8**, 1080-1094.

Willmott, A.J. and Mysak, L.A., 1980. Atmospherically forced eddies in the Northeast Pacific, *J. Phys. Oceanogr.*, **10**, 1769-1791.